1

Fundamental Enhancement Techniques

Raman B. Paranjape
University of Regina

1 Introduction

Image enhancement techniques are used to refine a given image, so that desired image features become easier to perceive for the human visual system or more likely to be detected by automated image analysis systems [1, 13]. Image enhancement allows the observer to see details in images that may not be immediately observable in the original image. This may be the case, for example, when the dynamic range of the data and that of the display are not commensurate, when the image has a high level of noise or when contrast is insufficient [4, 5, 8, 9].

Fundamentally, image enhancement is the transformation or mapping of one image to another [10, 14]. This transformation is not necessarily one-to-one, so that two different input images may transform into the same or similar output images after enhancement. More commonly, one may want to generate multiple enhanced versions of a given image. This aspect also means that enhancement techniques may be irreversible.

Often the enhancement of certain features in images is accompanied by undesirable effects. Valuable image information may be lost or the enhanced image may be a poor representation of the original. Furthermore, enhancement algorithms cannot be expected to provide information that is not present in the original image. If the image does not contain the feature to be enhanced, noise or other unwanted image components may be inadvertently enhanced without any benefit to the user.

In this chapter we present established image enhancement algorithms commonly used for medical images. Initial concepts and definitions are presented in Section 2. Pixel-based enhancement techniques described in Section 3 are transformations applied to each pixel without utilizing specifically the information in the neighborhood of the pixel. Section 4 presents enhancement with local operators that modify the value of each pixel using the pixels in a local neighborhood. Enhancement that can be achieved with multiple images of the same scene is outlined in Section 5. Spectral domain filters that can be used for enhancement are presented in Section 6. The techniques described in this chapter are applicable to dental and medical images as illustrated in the figures.

2 Preliminaries and Definitions

We define a digital image as a two-dimensional array of numbers that represents the real, continuous intensity distribution of a spatial signal. The continuous spatial signal is sampled at regular intervals and the intensity is quantized to a finite number of levels. Each element of the array is referred to as a picture element or pixel. The digital image is defined as a spatially distributed intensity signal $f(m, n)$, where f is the intensity of the pixel, and m and n define the position of the pixel along a pair of orthogonal axes usually defined as horizontal and vertical. We shall assume that the image has M rows and N columns and that the digital image has P quantized levels of intensity (gray levels) with values ranging from 0 to $P-1$.

The histogram of an image, commonly used in image enhancement and image characterization, is defined as a vector that contains the count of the number of pixels in the image at each gray level. The histogram, $h(i)$, can be defined as

$$h(i) = \sum_{m=0}^{M-1} \sum_{n=0}^{N-1} \delta(f(m, n) - i), \qquad i = 0, 1, \ldots, P-1,$$

where

$$\delta(w) = \begin{cases} 1 & w = 0, \\ 0 & \text{otherwise.} \end{cases}$$

A useful image enhancement operation is convolution using local operators, also known as kernels. Considering a kernel $w(k, l)$ to be an array of $(2K + 1 \times 2L + 1)$ coefficients where the point $(k, l) = (0, 0)$ is the center of the kernel, convolution of the image with the kernel is defined by:

$$g(m, n) = w(k, l) * f(m, n) = \sum_{k=-K}^{K} \sum_{l=-L}^{L} w(k, l) \cdot f(m-k, n-l),$$

where $g(m, n)$ is the outcome of the convolution or output image. To convolve an image with a kernel, the kernel is centered on an image pixel (m, n), the point-by-point products of the kernel coefficients and corresponding image pixels are obtained, and the subsequent summation of these products is used as the pixel value of the output image at (m, n). The complete output image $g(m, n)$ is obtained by repeating the same operation on all pixels of the original image [4, 5, 13]. A convolution kernel can be applied to an image in order to effect a specific enhancement operation or change in the image characteristics. This typically results in desirable attributes being amplified and undesirable attributes being suppressed. The specific values of the kernel coefficients depend on the different types of enhancement that may be desired.

Attention is needed at the boundaries of the image where parts of the kernel extend beyond the input image. One approach is to simply use the portion of the kernel that overlaps the input image. This approach can, however, lead to artifacts at the boundaries of the output image. In this chapter we have chosen to simply not apply the filter in parts of the input image where the kernel extends beyond the image. As a result, the output images are typically smaller than the input image by the size of the kernel.

so, if the size of the image is (6x7) and we are convoluting with a (3x3) filter, the output size according to the above rule will be (6-3+1x7-3+1) = (4,5)

https://plus.maths.org/content/fourier-transforms-images

The Fourier transform $F(u, v)$ of an image $f(m, n)$ is defined as

$$F(u, v) = \frac{1}{MN} \sum_{m=0}^{M-1} \sum_{n=0}^{N-1} f(m, n) e^{-2\pi j\left(\frac{um}{M} + \frac{vn}{N}\right)},$$
$$u = 0, 1, 2, \ldots, M-1 \quad v = 0, 1, 2, \ldots, N-1,$$

where u and v are the spatial frequency parameters. The Fourier transform provides the spectral representation of an image, which can be modified to enhance desired properties. A spatial-domain image can be obtained from a spectral-domain image with the inverse Fourier transform given by

$$f(m, n) = \sum_{u=0}^{M-1} \sum_{v=0}^{N-1} F(u, v) e^{2\pi j\left(\frac{um}{M} + \frac{vn}{N}\right)},$$
$$m = 0, 1, 2, \ldots, M-1, \quad n = 0, 1, 2, \ldots, N-1.$$

The forward or inverse Fourier transform of an $N \times N$ image, computed directly with the preceding definitions, requires a number of complex multiplications and additions proportional to N^2. By decomposing the expressions and eliminating redundancies, the fast Fourier transform (FFT) algorithm reduces the number of operations to the order of $N \log_2 N$ [5]. The computational advantage of the FFT is significant and increases with increasing N. When $N = 64$ the number of operations are reduced by an order of magnitude and when $N = 1024$, by two orders of magnitude.

Todo: Analyze the Fourier Transform of an Image with different angles of symmetry.

3 Pixel Operations

In this section we present methods of image enhancement that depend only upon the pixel gray level and do not take into account the pixel neighborhood or whole-image characteristics.

3.1 Compensation for Nonlinear Characteristics of Display or Print Media

Digital images are generally displayed on cathode ray tube (CRT) type display systems or printed using some type of photographic emulsion. Most display mechanisms have nonlinear intensity characteristics that result in a nonlinear intensity profile of the image when it is observed on the display. This effect can be described succinctly by the equation

$$e(m, n) = C(f(m, n)),$$

where $f(m, n)$ is the acquired intensity image, $e(m, n)$ represents the actual intensity output by the display system, and $C()$ is a nonlinear display system operator. In order to correct for the nonlinear characteristics of the display, a transform that is the inverse of the display's nonlinearity must be applied [14, 16].

$$g(m,n) = T(e(m,n)) \cong C^{-1}(C(f(m,n)))$$

$$g(m,n) \cong f(m,n),$$

where $T()$ is a nonlinear operator which is approximately equal to $C^{-1}()$, the inverse of the display system operator, and $g(m,n)$ is the output image.

Determination of the characteristics of the nonlinearity could be difficult in practice. In general, if a linear intensity wedge is imaged, one can obtain a test image that captures the complete intensity scale of the image acquisition system. However, an intensity measurement device that is linear is then required to assess the output of the display system, in order to determine its actual nonlinear characteristics.

A slightly exaggerated example of this type of a transform is presented in Fig.1. Figure 1a presents a simulated CRT display with a logarithmic characteristic. This characteristic tends to suppress the dynamic range of the image decreasing the contrast. Figure 1b presents the same image after an inverse transformation to correct for the display nonlinearity. Although these operations do in principle correct for the display, the primary mechanism for review and analysis of image information is the human visual system, which is fundamentally a nonlinear reception system and adapts locally to the intensities presented.

TD: Histogram of small and large dynamic range of images and how to increase the contrast. (use the same image for histogram)

3.2 Intensity Scaling

Intensity scaling is a method of image enhancement that can be used when the dynamic range of the acquired image data significantly exceeds the characteristics of the display system, or vice versa. It may also be the case that image information is present in specific narrow intensity bands that may be of special interest to the observer. Intensity scaling allows the observer to focus on specific intensity bands in the image by modifying the image such that the intensity band of interest spans the dynamic range of the display [14, 16]. For example, if f_1 and f_2 are known to define the intensity band of interest, a scaling transformation may be defined as

$$e = \begin{cases} f & f_1 \le f \le f_2 \\ 0 & \text{otherwise} \end{cases}$$

$$g = \left\{ \frac{e - f_1}{f_2 - f_1} \right\} \cdot (f_{\max}),$$

where e is an intermediate image, g is the output image, and $f_{\max}$ is the maximum intensity of the display.

These operations may be seen through the images in Fig. 2. Figure 2a presents an image with detail in the intensity band from 90 to 170 that may be of interest to, for example a gum specialist. The image, however, is displayed such that all gray levels in the range 0 to 255 are seen. Figure 2b shows the histogram of the input image and Fig. 2c presents the same image with the 90-to-170 intensity band stretched across the output band of the display. Figure 2d shows the histogram of the output image with the intensities that were initially between 90 and 170, but are now stretched over the range 0 to 255. The detail in the narrow band is now easily perceived; however, details outside the band are completely suppressed.

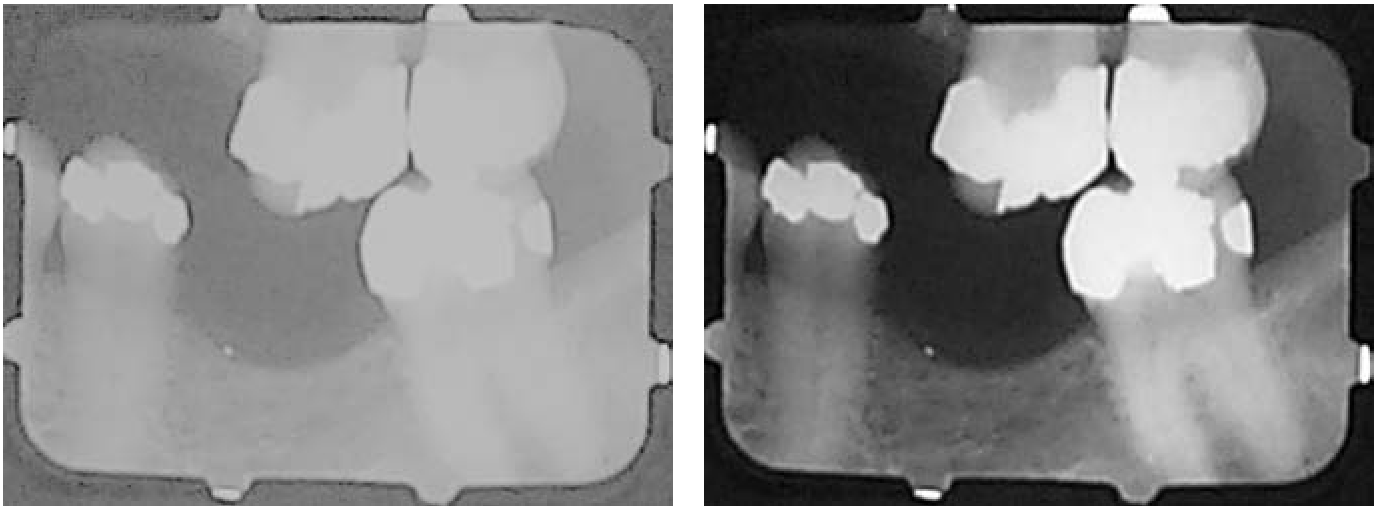

(a) (b)

FIGURE 1 (a) Original image as seen on a poor-quality CRT-type display. This image has poor contrast, and details are difficult to perceive—especially in the brighter parts of the image such as in areas with high tooth density or near filling material. (b) The nonlinearity of the display is reversed by the transformation, and structural details become more visible. Details within the image such as the location of amalgam, the cavity preparation liner, tooth structures, and bony structures are better visualized.

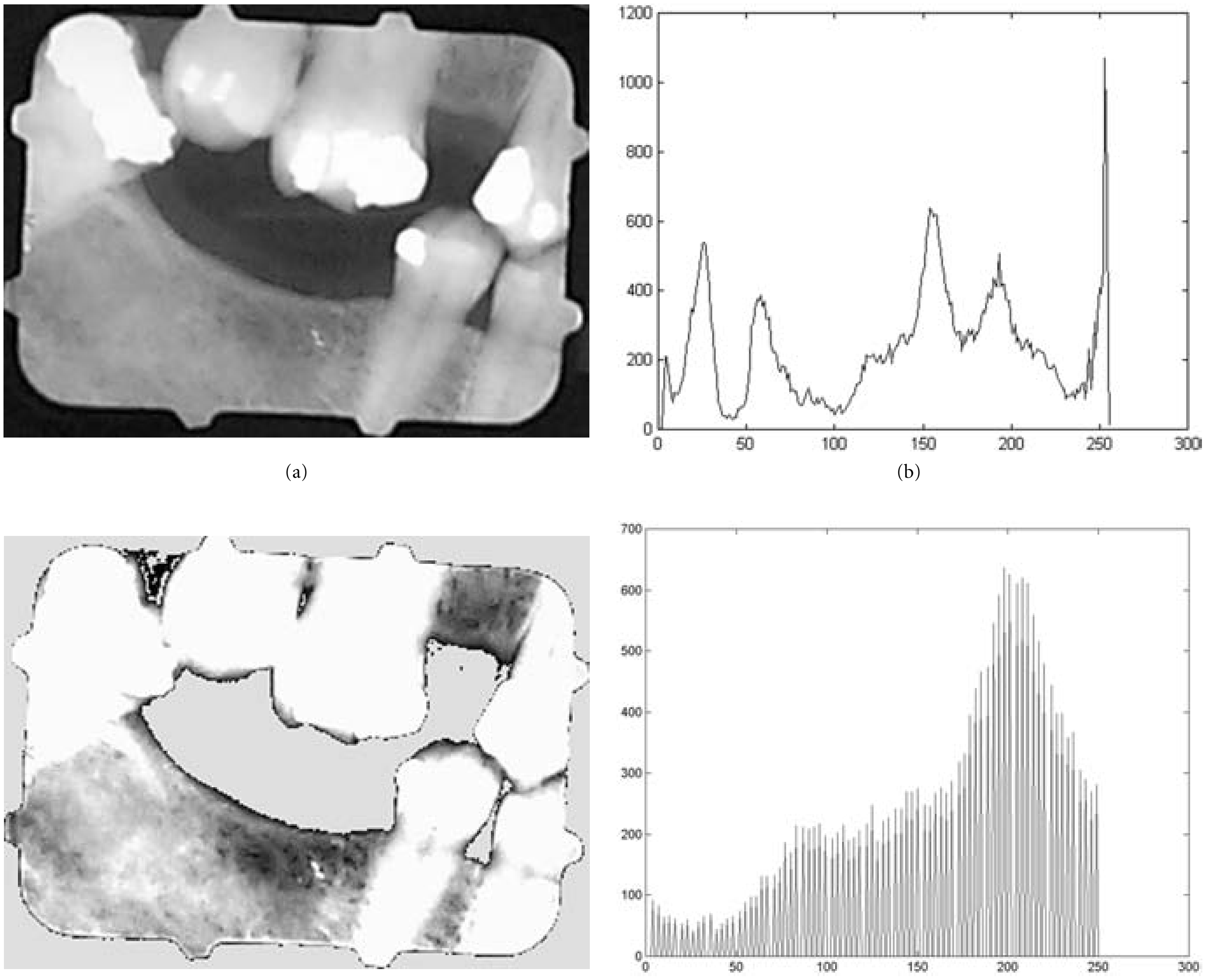

(a) (b) (c) (d)

FIGURE 2 (a) Input image where details of interest are in the 90-to-170 gray level band. This intensity band identifies the bony structures in this image and provides an example of a feature that may be of dental interest. (b) Histogram of the input image in (a). (c) This output image selectively shows the intensity band of interest stretched over the entire dynamic range of the display. This specific enhancement may be potentially useful in highlighting features or characteristics of bony tissue in dental X-ray imagery. This technique may be also effective in focusing attention on other image features such as bony lamina dura or recurrent caries. (d) Histogram of the output image in (c). This histogram shows the gray levels in the original image in the 90-to-170 intensity band stretched over 0 to 255.

TD: Intensity Scaling to observe if the features are getting highlighted more using different values of f max

3.3 Histogram Equalization

Although intensity scaling can be very effective in enhancing image information present in specific intensity bands, often information is not available *a priori* to identify the useful intensity bands. In such cases, it may be more useful to maximize the information conveyed from the image to the user by distributing the intensity information in the image as uniformly as possible over the available intensity band [3, 6, 7].

This approach is based on an approximate realization of an information-theoretic approach in which the normalized histogram of the image is interpreted as the probability density function of the intensity of the image. In histogram equalization, the histogram of the input image is mapped to a new maximally-flat histogram.

As indicated in Section 2, the histogram is defined as $h(i)$, with 0 to $P-1$ gray levels in the image. The total number of pixels in the image, $M*N$, is also the sum of all the values in $h(i)$. Thus, in order to distribute most uniformly the intensity profile of the image, each bin of the histogram should have a pixel count of $(M * N)/P$.

It is, in general, possible to move the pixels with a given intensity to another intensity, resulting in an increase in the pixel count in the new intensity bin. On the other hand, there is no acceptable way to reduce or divide the pixel count at a specific intensity in order to reduce the pixel count to the desired $(M * N)/P$. In order to achieve approximate uniformity, the average value of the pixel count over a number of pixel values can be made close to the uniform level.

A simple and readily available procedure for redistribution of the pixels in the image is based on the normalized cumulative histogram, defined as

$$H(j) = \frac{1}{M \cdot N} \sum_{i=0}^{j} h(i), \qquad j = 0, 1, \ldots P - 1.$$

The normalized cumulative histogram can be used as a mapping between the original gray levels in the image and the new gray levels required for enhancement. The enhanced image $g(m, n)$ will have a maximally uniform histogram if it is defined as

$$g(m, n) = (P - 1) \cdot H(f(m, n)).$$

Figure 3a presents an original dental image where the gray levels are not uniformly distributed, while the associated histogram and cumulative histogram are shown in Figs 3b and 3c, respectively. The cumulative histogram is then used to map the gray levels of the input images to the output image shown in Fig. 3d. Figure 3e presents the histogram of Fig. 3d, and Fig. 3f shows the corresponding cumulative histogram. Figure 3f should ideally be a straight line from $(0, 0)$ to $(P - 1, P - 1)$, but in fact only approximates this line to the extent possible given the initial distribution of gray levels. Figure 3g through 1 show the enhancement of a brain MRI image with the same steps as above.

4 Local Operators

Local operators enhance the image by providing a new value for each pixel in a manner that depends only on that pixel and others in a neighborhood around it. Many local operators are linear spatial filters implemented with a kernel convolution, some are nonlinear operators, and others impart histogram equalization within a neighborhood. In this section we present a set of established standard filters commonly used for enhancement. These can be easily extended to obtain slightly modified results by increasing the size of the neighborhood while maintaining the structure and function of the operator.

4.1 Noise Suppression by Mean Filtering

Mean filtering can be achieved by convolving the image with a $(2K + 1 \times 2L + 1)$ kernel where each coefficient has a value equal to the reciprocal of the number of coefficients in the kernel. For example, when $L = K = 1$, we obtain

$$w(k, l) = \begin{Bmatrix} 1/9 & 1/9 & 1/9 \\ 1/9 & 1/9 & 1/9 \\ 1/9 & 1/9 & 1/9 \end{Bmatrix},$$

referred to as the 3×3 averaging kernel or mask. Typically, this type of smoothing reduces noise in the image, but at the expense of the sharpness of edges [4, 5, 12, 13]. Examples of the application of this kernel are seen in Fig. 4(a–d). Note that the size of the kernel is a critical factor in the successful application of this type of enhancement. Image details that are small relative to the size of the kernel are significantly suppressed, while image details significantly larger than the kernel size are affected moderately. The degree of noise suppression is related to the size of the kernel, with greater suppression achieved by larger kernels.

4.2 Noise Suppression by Median Filtering

Median filtering is a common nonlinear method for noise suppression that has unique characteristics. It does not use convolution to process the image with a kernel of coefficients. Rather, in each position of the kernel frame, a pixel of the input image contained in the frame is selected to become the output pixel located at the coordinates of the kernel center. The kernel frame is centered on each pixel (m, n) of the original image, and the median value of pixels within the kernel frame is computed. The pixel at the coordinates (m, n) of the output image is set to this median value. In general, median filters do not have the same smoothing characteristics as the mean filter [4, 5, 8, 9, 15]. Features that are smaller than half the size of the median filter kernel are completely removed by the filter. Large discontinuities such as edges and large changes in image intensity are not affected in terms of gray level intensity by the median filter, although their positions may be shifted by a few pixels. This nonlinear operation of the median filter allows significant reduction of specific types of noise. For example, "shot noise" may be removed completely from an image without attenuation of significant edges or image characteristics. Figure 5 presents typical results of median filtering.

4.3 Edge Enhancement

Edge enhancement in images is of unique importance because the human visual system uses edges as a key factor in the comprehension of the contents of an image [2, 4, 5, 10,13, 14]. Edges in different orientations can be selectively identified and

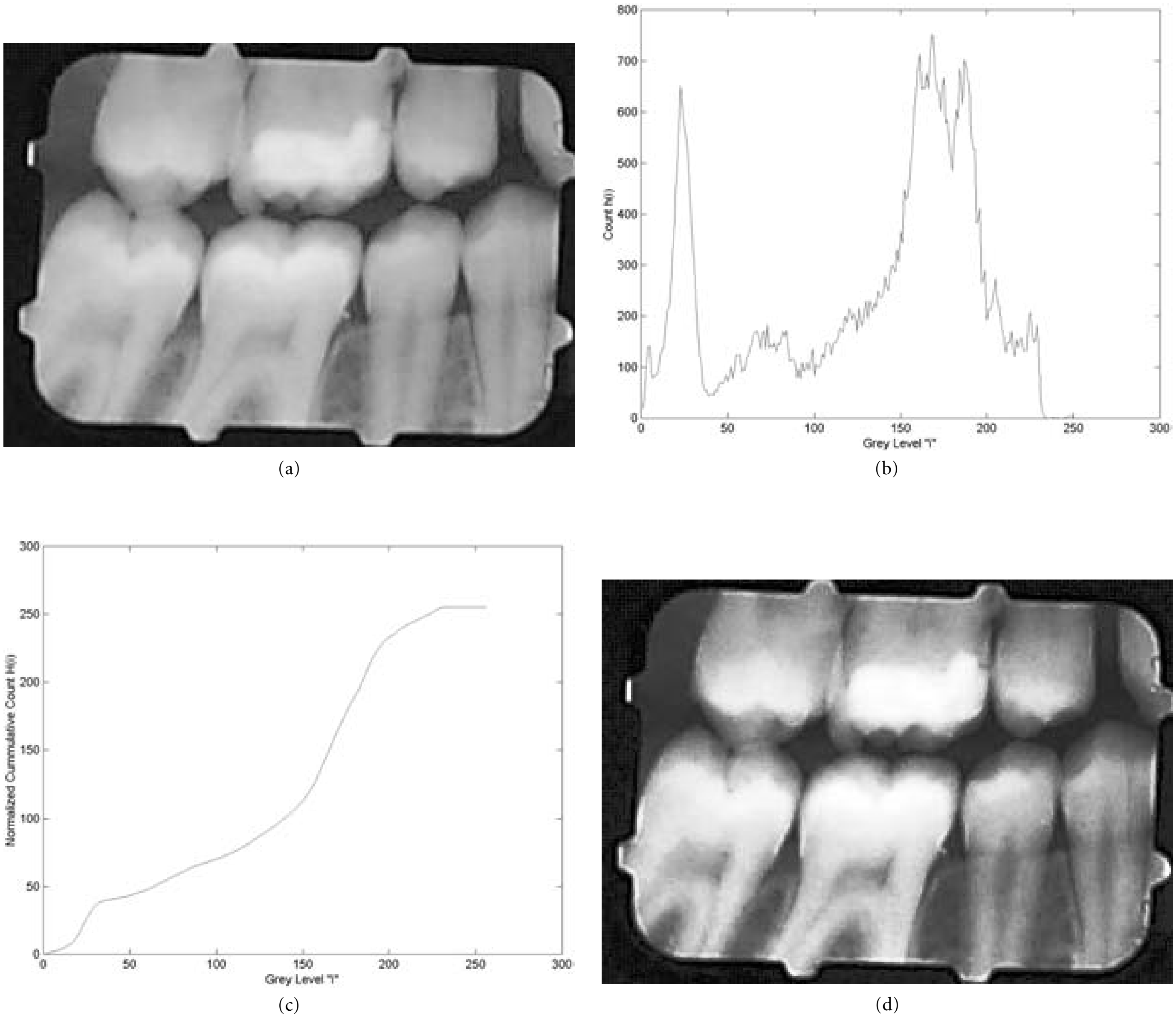

FIGURE 3 (a) Original image where gray levels are not uniformly distributed. Many image details are not well visualized in this image because of the low contrast. (b) Histogram of the original image in (a). Note the nonuniformity of the histogram. (c) Cumulative histogram of the original image in (a). (d) Histogram-equalized image. Contrast is enhanced so that subtle changes in intensity are more readily observable. This may allow earlier detection of pathological structures. (e) Histogram of the enhanced image in (d). Note that the distribution of intensity counts that are greater than the mean value have been distributed over a larger gray level range. (f) Cumulative histogram of the enhanced image in (d). (g) Original brain MRI image (courtesy of Dr. Christos Dzavatzikos, Johns Hopkins Radiology Department). (h) through (l) same steps as above for brain image.

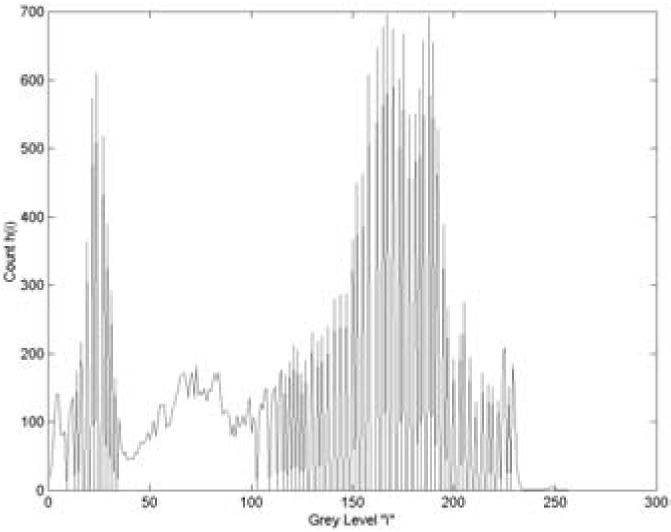

(e)

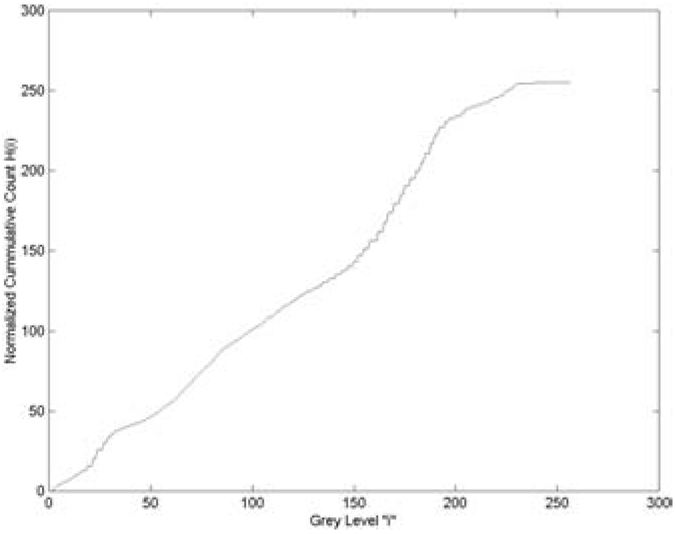

(f)

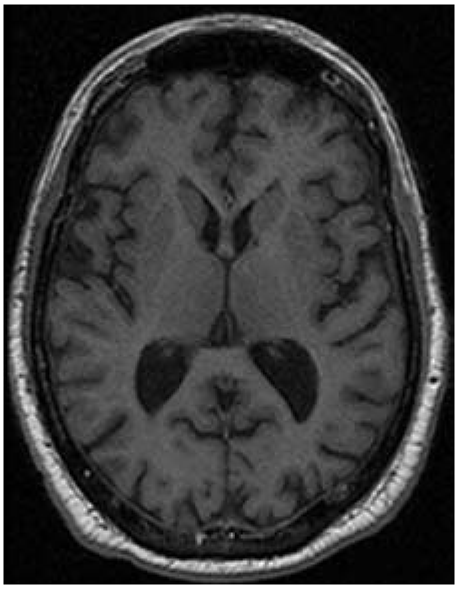

(g)

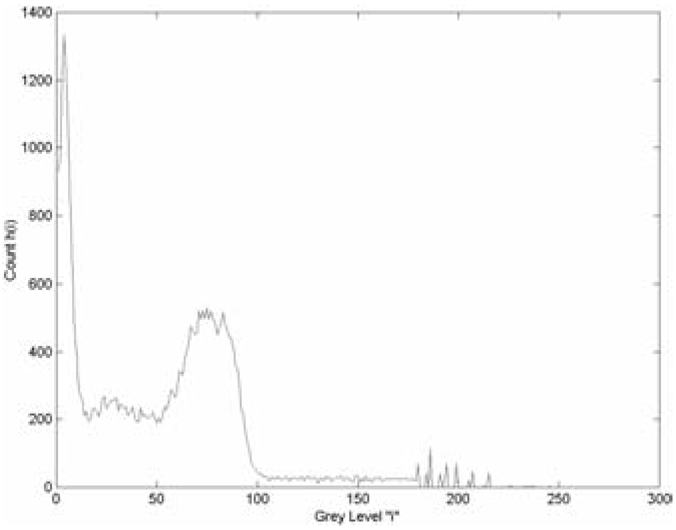

(h)

FIGURE 3 (Continued).

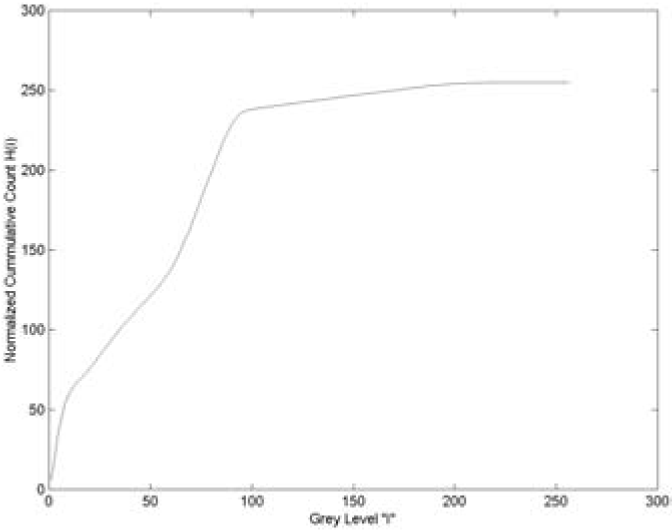

(i)

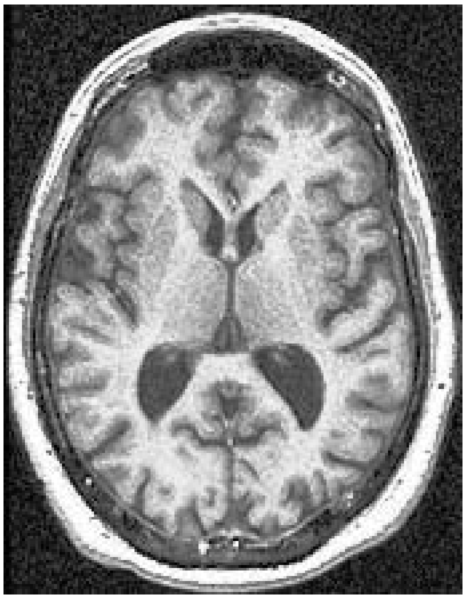

(j)

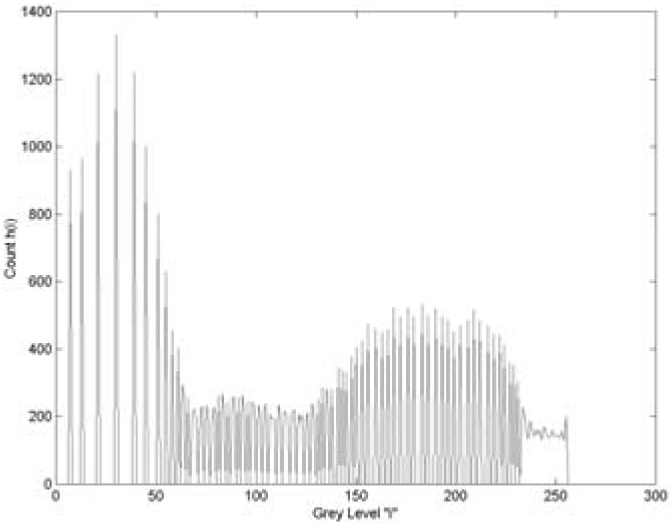

(k)

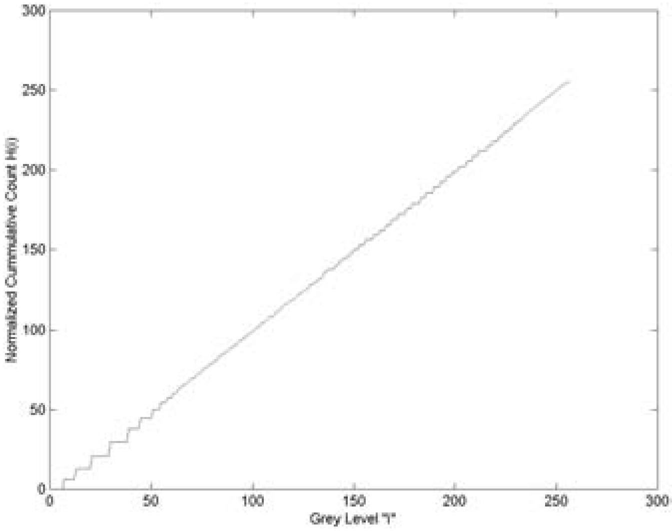

(l)

FIGURE 3 (Continued).

enhanced. The edge-enhanced images may be combined with the original image in order to preserve the context.

Horizontal edges and lines are enhanced with

$$w_{H1}(k,l) = \begin{Bmatrix} 1 & 1 & 1 \\ 0 & 0 & 0 \\ -1 & -1 & -1 \end{Bmatrix} \quad \text{or} \quad w_{H2}(k,l) = \begin{Bmatrix} -1 & -1 & -1 \\ 0 & 0 & 0 \\ 1 & 1 & 1 \end{Bmatrix},$$

and vertical edges and lines are enhanced with

$$w_{V1}(k,l) = \begin{Bmatrix} 1 & 0 & -1 \\ 1 & 0 & -1 \\ 1 & 0 & -1 \end{Bmatrix} \quad \text{or} \quad w_{V2}(k,l) = \begin{Bmatrix} -1 & 0 & 1 \\ -1 & 0 & 1 \\ -1 & 0 & 1 \end{Bmatrix}.$$

The omnidirectional kernel (unsharp mask) enhances edges in all directions:

$$K_{HP}(k,l) = \begin{Bmatrix} -1/8 & -1/8 & -1/8 \\ -1/8 & 1 & -1/8 \\ -1/8 & -1/8 & -1/8 \end{Bmatrix}.$$

Note that the application of these kernels to a positive-valued

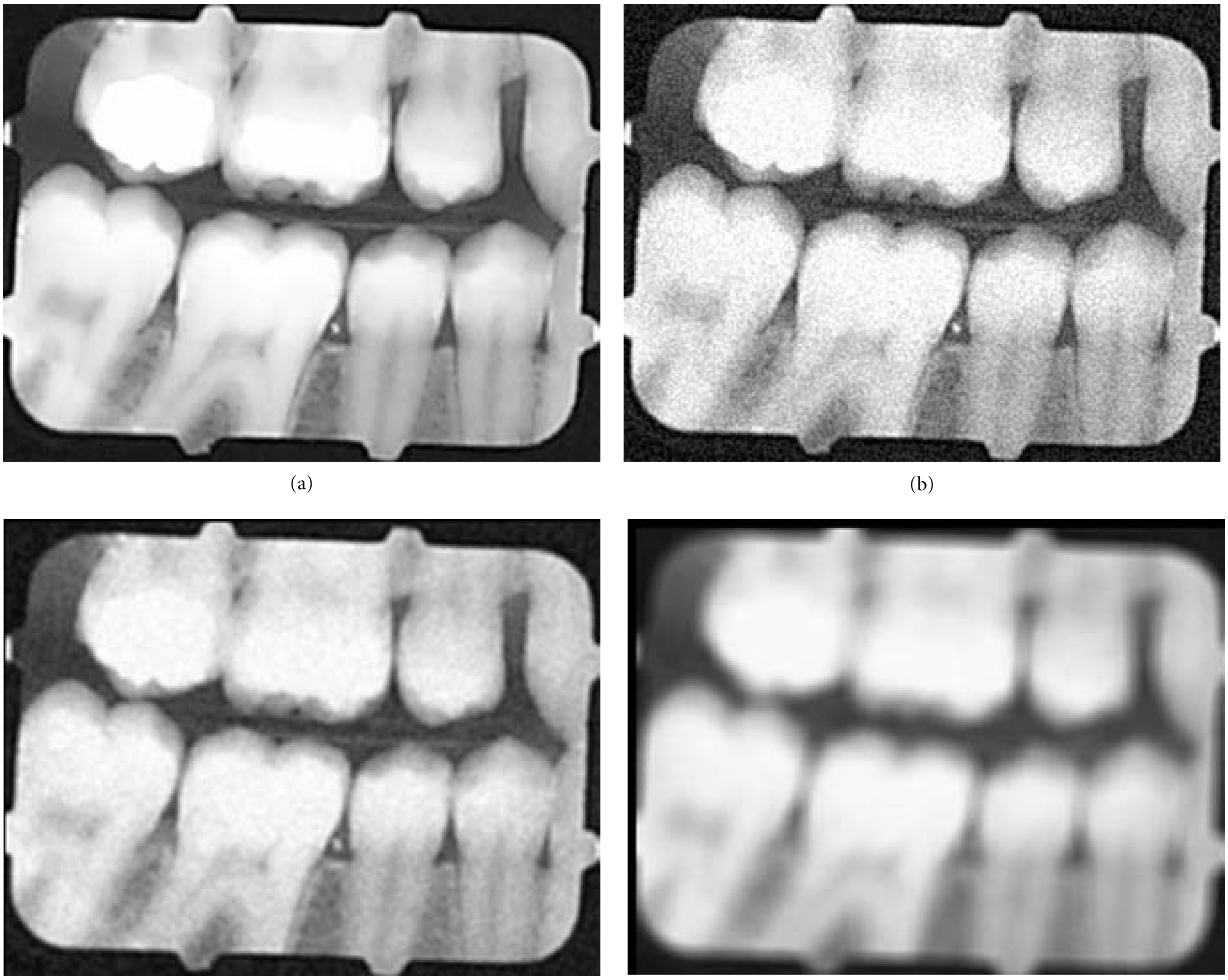

(a) (b) (c) (d)

FIGURE 4 (a) Original bitewing X-ray image. (b) Original image in (a) corrupted by added Gaussian white noise with maximum amplitude of ± 25 gray levels. (c) Image in (b) convolved with the 3×3 mean filter. The mean filter clearly removes some of the additive noise; however, significant blurring also occurs. This image would not have significant clinical value. (d) Image in (b) convolved with the 9×9 mean filter. This filter has removed almost all of the effects of the additive noise. However, the usefulness of this filter is limited because the filter size is similar to that of significant structures within the image, causing severe blurring.

image can result in an output image with both positive and negative values. An enhanced image with only positive pixels can be obtained either by adding an offset or by taking the absolute value of each pixel in the output image. If we are interested in displaying edge-only information, this may be a good approach. On the other hand, if we are interested in enhancing edges that are consistent with the kernel and suppressing those that are not, the output image may be added to the original input image. This addition will most likely result in a nonnegative image.

Figure 6 illustrates enhancement after the application of the kernels w_{H1}, w_{V1}, and w_{HP} to the image in Fig. 3a and 3g. Figures 6a, b, and c show the absolute value of the output images obtained with w_{H1}, w_{V1}, and w_{HP}, respectively applied to the dental image while 6d, e, and f show the same for the brain image. In Fig. 7, the outputs obtained with these three kernals are added to the original images of Fig. 3a and g. In this manner the edge information is enhanced while retaining the context information of the original image. This is accomplished in one step by

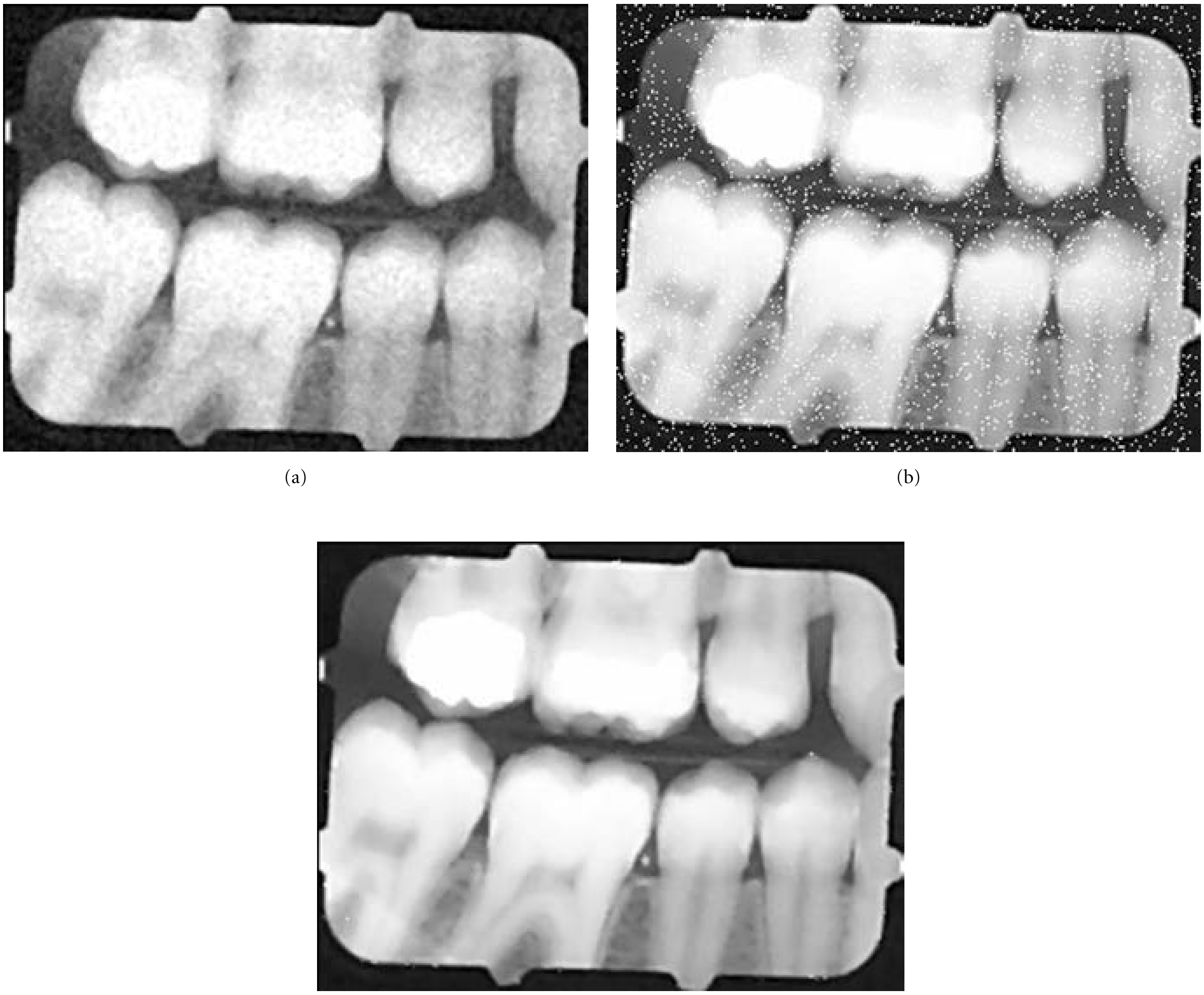

(a) (b)

(c)

FIGURE 5 (a) Image in Fig. 4b enhanced with a 3×3 median filter. The median filter is not as effective in noise removal as the mean filter of the same size; however, edges are not as severely degraded by the median filter. (b) Image in Fig. 4a with added shot noise. (c) Image in figure 5(b) enhanced by a 3×3 median filter. The median filter is able to significantly enhance this image, allowing almost all shot noise to be eliminated. This image has good diagnostic value.

convolving the original image with the kernel after adding 1 to its central coefficient. Edge enhancement appears to provide greater contrast than the original imagery when diagnosing pathologies.

Edges can be enhanced with several edge operators other than those just mentioned and illustrated. Some of these are described in the chapter entitled "Overview and Fundamentals of Medical Image Segmentation," since they also form the basis for edge-based segmentation.

4.4 Local-Area Histogram Equalization

A remarkably effective method of image enhancement is local-area histogram equalization, obtained with a modification of the pixel operation defined in Section 3.3. Local-area histogram equalization applies the concepts of whole-image histogram equalization to small, overlapping local areas of the image [7, 11]. It is a nonlinear operation and can significantly increase the observability of subtle features in

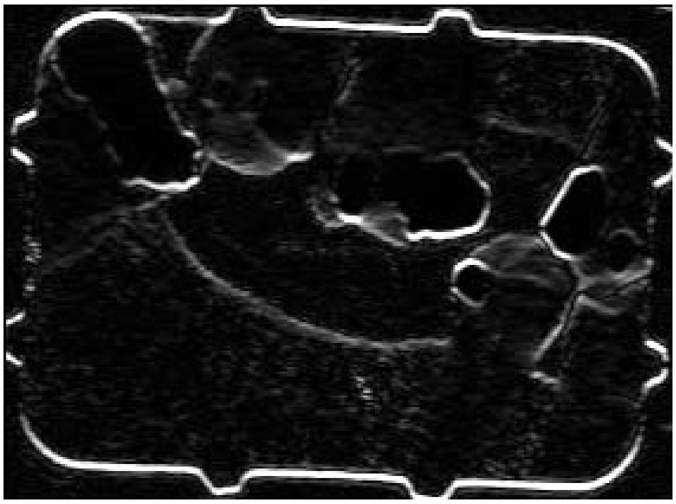

(a)

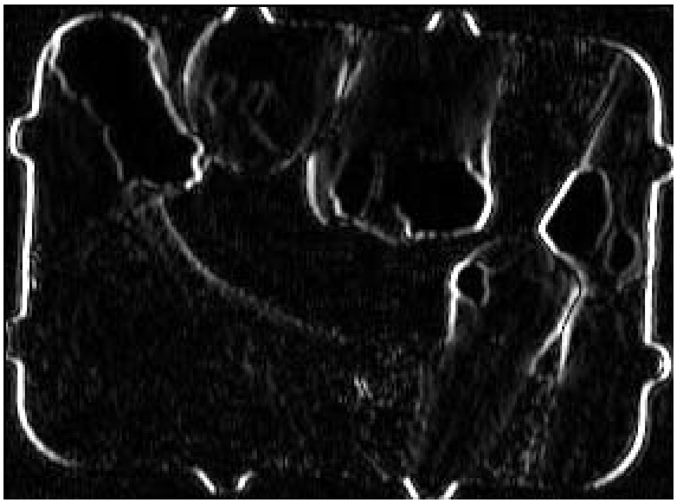

(b)

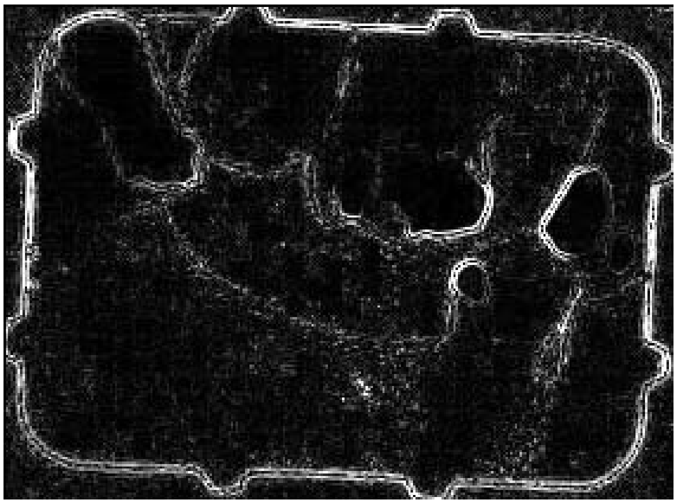

(c)

FIGURE 6 (a) Absolute value of output image after convolution of w_{H1} with the image in Fig. 3a. (b) Absolute value of output image after convolution of w_{V1} with the image in Fig. 3a. (c) Absolute value of output image after convolution of w_{HP}. (d through f) same as a, b, and c using image in Fig. 3g.

(d)

(e)

(f)

(a)

(b)

(c)

FIGURE 7 (a) Sum of original image in Fig. 3a and its convolution with w_{H1}, (b) with w_{V1}, and (c) with w_{HP}. (d through f) same as a, b, and c using image in Fig. 3g.

(d)

(e)

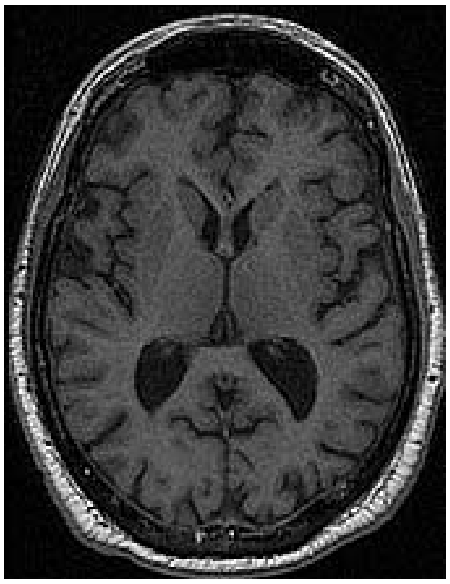

(f)

the image. The method formulated as shown next is applied at each pixel (m, n) of the input image.

$$h_{LA}(m,n)(i) = \sum_{k=-K}^{K} \sum_{l=-L}^{L} \delta(f(m+l, n+k) - i), \quad i = 0, 1, \ldots P-1$$

$$H_{LA}(m,n)(j) = \frac{1}{(2K+1)\cdot(2L+1)} \sum_{i=0}^{j} h_{LA}(m,n)(i), \quad j = 0, 1, \ldots P-1$$

$$g(m,n) = (P-1)\cdot H_{LA}(m,n)(f(m,n))$$

where $h_{LA}(m,n)(i)$ is the local-area histogram, $H_{LA}(m,n)(j)$ is the local-area cumulative histogram, and $g(m,n)$ is the output image. Figure 8 shows the output image obtained by enhancing the image in Fig.2a with local-area histogram equalization using $K = L = 15$ or a 31×31 kernel size.

Local-area histogram equalization is a computationally intensive enhancement technique. The computational complexity of the algorithm goes up as the square of the size of the kernel. It should be noted that since the transformation that is applied to the image depends on the local neighborhood only, each pixel is transformed in a unique way. This results in higher visibility for hidden details spanning very few pixels in relation to the size of the full image. A significant limitation of this method is that the mapping between the input and output images is nonlinear and highly nonmonotonic. This means that it is inappropriate to make quantitative measurements of pixel intensity on the output image, as the same gray level may be transformed one way in one part of the image and a completely different way in another part.

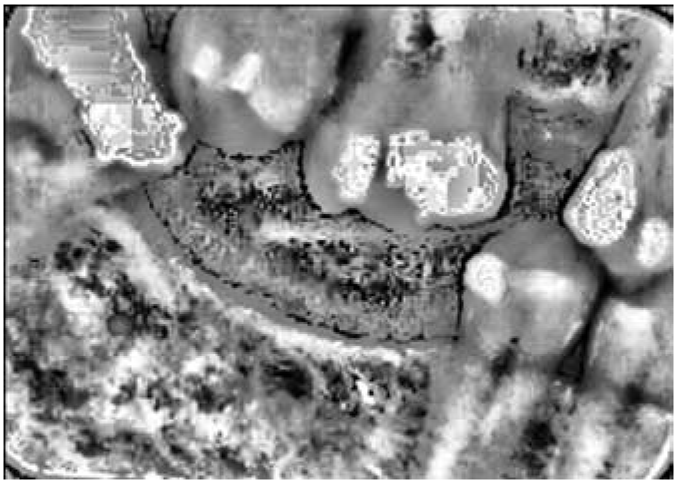

FIGURE 8 Output image obtained when local-area histogram equalization was applied to the image in Fig. 2a. Note that the local-area histogram equalization produces very high-contrast images, emphasizing detail that may otherwise be imperceptible. This type of enhancement is computationally very intensive and it may be useful only for discovery purposes to determine if any evidence of a feature exists.

5 Operations with Multiple Images

This section outlines two enhancement methods that require more than one image of the same scene. In both methods, the images have to be registered and their dynamic ranges have to be comparable to provide a viable outcome.

5.1 Noise Suppression by Image Averaging

Noise suppression using image averaging relies on three basic assumptions: (1) that a relatively large number of input images are available, (2) that each input image has been corrupted by the same type of additive noise, and (3) that the additive noise is random with zero mean value and independent of the image. When these assumptions hold, it may be advantageous to acquire multiple images with the specific purpose of using image averaging [1] since with this approach even severely corrupted images can be significantly enhanced. Each of the noisy images $a_i(m,n)$ can be represented by

$$a_i(m,n) = f(m,n) + d_i(m,n),$$

where $f(m,n)$ is the underlying noise-free image, and $d_i(m,n)$ is the additive noise in that image. If a total of Q images are available, the averaged image is

$$g(m,n) = \frac{1}{Q}\sum_{i=1}^{Q} a_i(m,n)$$

such that

$$E\{g(m,n)\} = f(m,n)$$

and

$$\sigma_g = \frac{\sigma_d}{\sqrt{Q}},$$

where E{ $\cdot$ } is the expected value operator, σ_g is the standard deviation of $g(m,n)$, and σ_d is that of the noise. Noise suppression is more effective for larger values of Q.

5.2 Change Enhancement by Image Subtraction

Image subtraction is generally performed between two images that have significant similarities between them. The purpose of image subtraction is to enhance the differences between two images (1). Images that are not captured under the same or very similar conditions may need to be registered [17]. This may be the case if the images have been acquired at different times or under different settings. The output image may have a very small dynamic range and may need to be rescaled to the available display range. Given two images $f_1(m,n)$ and $f_2(m,n)$, the rescaled output image $g(m,n)$ is obtained with

$$b(m,n) = f_1(m,n) - f_2(m,n)$$

$$g(m,n) = f_{\max} \cdot \left(\frac{b(m,n) - \min\{b(m,n)\}}{\max\{b(m,n)\} - \min\{b(m,n)\}} \right)$$

where $f_{\max}$ is the maximum gray level value available, $b(m,n)$ is the unstretched difference image, and $\min\{b(m,n)\}$ and $\max\{b(m,n)\}$ are the minimal and maximal values in $b(m,n)$, respectively.

find the difference between images.

6 Frequency Domain Techniques

Linear filters used for enhancement can also be implemented in the frequency domain by modifying the Fourier transform of the original image and taking the inverse Fourier transform. When an image $g(m,n)$ is obtained by convolving an original image $f(m,n)$ with a kernel $w(m,n)$,

$$g(m,n) = w(m,n) * f(m,n),$$

the convolution theorem states that $G(u,v)$, the Fourier transform of $g(m,n)$, is given by

$$G(u,v) = W(u,v)F(u,v),$$

where $W(u,v)$ and $F(u,v)$ are the Fourier transforms of the kernel and the image, respectively. Therefore, enhancement can be achieved directly in the frequency domain by multiplying $F(u,v)$, pixel-by-pixel, by an appropriate $W(u,v)$ and forming the enhanced image with the inverse Fourier transform of the product. Noise suppression or image smoothing can be obtained by eliminating the high-frequency components of $F(u,v)$, while edge enhancement can be achieved by eliminating its low-frequency components. Since the spectral filtering process depends on a selection of frequency parameters as high or low, each pair (u,v) is quantified with a measure of distance from the origin of the frequency plane,

$$D(u,v) = \sqrt{u^2 + v^2},$$

which can be compared to a threshold D_T to determine if (u,v) is high or low. The simplest approach to image smoothing is the ideal low-pass filter $W_L(u,v)$, defined to be 1 when $D(u,v) \le D_T$ and 0 otherwise. Similarly, the ideal high-pass filter $W_H(u,v)$ can be defined to be 1 when $D(u,v) \ge D_T$ and 0 otherwise. However, these filters are not typically used in practice, because images that they produce generally have spurious structures that appear as intensity ripples, known as ringing [5]. The inverse Fourier transform of the rectangular window $W_L(u,v)$ or $W_H(u,v)$ has oscillations, and its convolution with the spatial-domain image produces the ringing. Because ringing is associated with the abrupt 1 to 0 discontinuity of the ideal filters, a filter that imparts a smooth transition between the desired frequencies and the attenuated ones is used to avoid ringing. The commonly used Butterworth low-pass and high-pass filters are defined respectively as

$$B_L(u,v) = \frac{1}{1 + c[D(u,v)/D_T]^{2n}}$$

and

$$B_H(u,v) = \frac{1}{1 + c[D_T/D(u,v)]^{2n}},$$

where c is a coefficient that adjusts the position of the transition and n determines its steepness. If $c = 1$, these two functions take the value 0.5 when $D(u,v) = D_T$. Another common choice for c is $\sqrt{2} - 1$, which yields 0.707 (-3 dB) at the cutoff D_T. The most common choice of n is 1; higher values yield steeper transitions.

The threshold D_T is generally set by considering the power of the image that will be contained in the preserved frequencies. The set S of frequency parameters (u,v) that belong to the preserved region, i.e., $D(u,v) \le D_T$ for low-pass and $D(u,v) \ge D_T$ for high-pass, determines the amount of retained image power. The percentage of total power that the retained power constitutes is given by

$$\beta = \frac{\sum_{(u,v)\in S} |F(u,v)|^2}{\sum_{\forall(u,v)} |F(u,v)|^2} \times 100$$

and is used generally to guide the selection of the cutoff threshold. In Fig. 9a, circles with radii r_β that correspond to five different β values are shown on the Fourier transform of an original MRI image in Fig. 9e. The $u = v = 0$ point of the transform is in the center of the image in Fig. 9a. The Butterworth low-pass filter obtained by setting D_T equal to r_β for $\beta = 90\%$, with $c = 1$ and $n = 1$, is shown in Fig. 9b where bright points indicate high values of the function. The corresponding filtered image in Fig. 9f shows the effects of smoothing. A high-pass Butterworth filter with D_T set at the 95% level is shown in Fig. 9d, and its output in Fig. 9h highlights the highest frequency components that form 5% of the image power. Figure 9c shows a band-pass filter formed by the conjunction of a low-pass filter at 95% and a high-pass filter at 75%, while the output image of this band-pass filter is in Fig. 9g.

7 Concluding Remarks

This chapter has focused on fundamental enhancement techniques used on medical and dental images. These techniques have been effective in many applications and are commonly used in practice. Typically, the techniques presented in this chapter form a first line of algorithms in attempts to

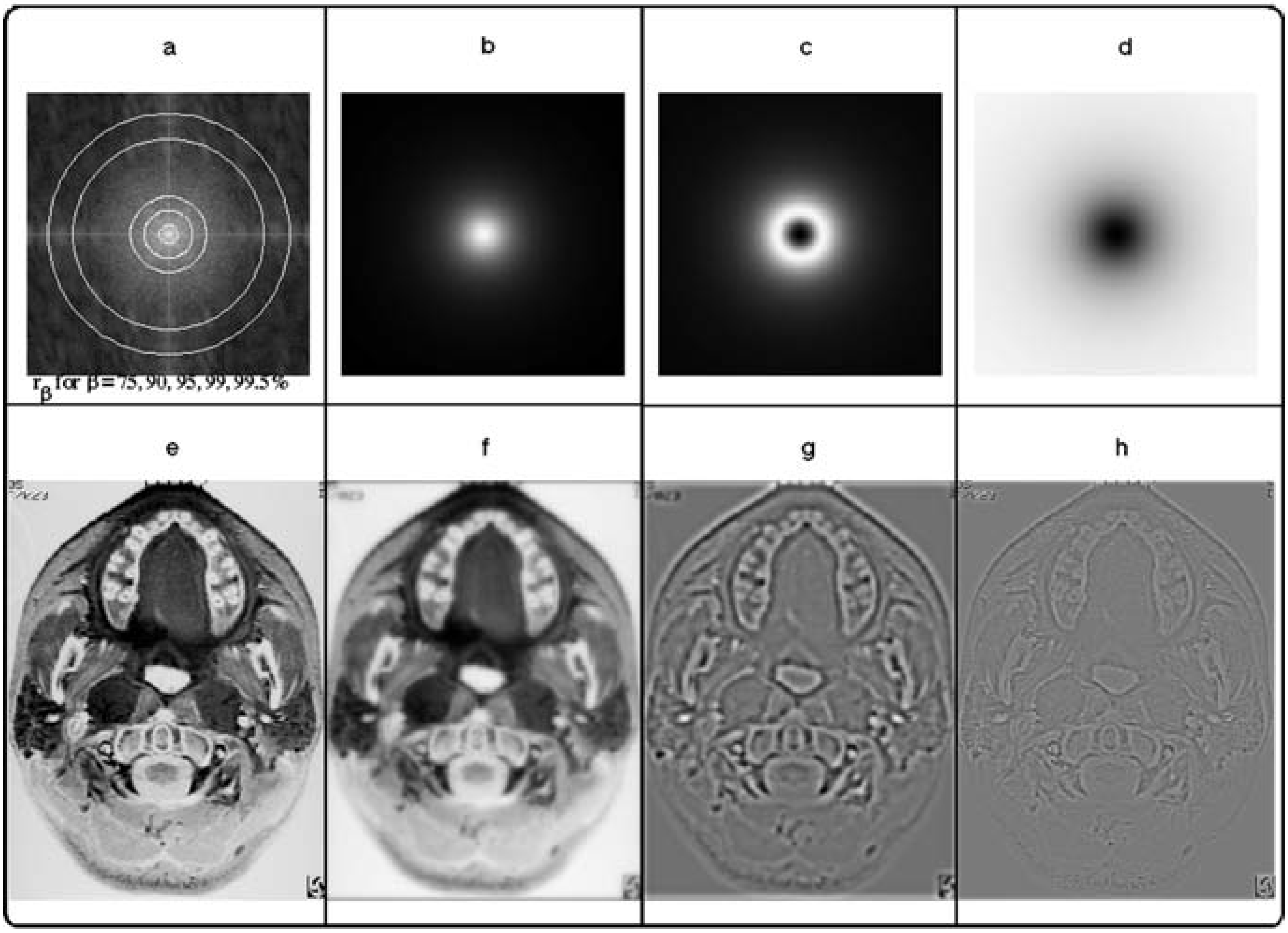

FIGURE 9 Filtering with the Butterworth filter. (a) Fourier transform of MRI image in (e); the five circles correspond to the β values 75, 90, 95, 99, and 99.5%. (b) Fourier transform of low-pass filter with $\beta = 90\%$ which provides the output image in (f). (c) Band-pass filter with band $\beta = 75\%$ to $\beta = 90\%$ whose output is in (g). (d) High-pass filter with $\beta = 95\%$, which yields the image in (h). (Courtesy of Dr. Patricia Murphy, Johns Hopkins University Applied Physics Laboratory.)

enhance image information. After these algorithms have been applied and adjusted for best outcome, additional image enhancement may be required to improve image quality further. Computationally more intensive algorithms may then be considered to take advantage of context-based and object-based information in the image. Examples and discussions of such techniques are presented in subsequent chapters.

Acknowledgments

The author thanks Dr. Bill Moyer for providing access to data and for discussions. Mr. Mark Sluser and Mr. Rick Yue supported this work. NSERC and the Government of Saskatchewan, Post Secondary Education, provided financial support for this project. TR*Labs* Regina provided laboratory facilities.

References

1. de Graaf, C. N., and Viergever, M. A. (ed.), *Information Processing in Medical Imaging.* Plenum Press, New York, 1988.
2. Fong, Y. S., Pomala-Roez, C. A., and Wong, X. H., Comparison study of non-linear filters in image processing applications. *Opti. Eng.* **28**(7), 749–760 (1989).
3. Frei, W., Image enhancement by image hyberbolization. *Comp. Graph. Image Process.* **6**, 286–294 (1977).

4. Gonzalez, R. C., and Wintz, P., *Digital Image Processing*. Addison-Wesley, Reading, MA, 1987.
5. Gonzalez, R. C., and Woods, R. E., *Digital Image Processing* Addison-Wesley, Reading, MA, 1992.
6. Hall, E. H. Almost uniform distributions from image enhancement, *IEEE Trans. Comp.* **C-23**(2), 207–208 (1974).
7. Ketchum, D. J., Real-time image enhancement techniques. *Proc. SPIE/OSA* **74**, 120–125 (1976).
8. Lewis, R., *Practical Digital Image Processing*. Ellis Horwood, West Sussex, UK, 1990.
9. Low, A., *Introduction to Computer Vision and Image Processing*. McGraw-Hill, U.K., 1991.
10. Niblack, W., *An Introduction to Digital Image Processing*. Prentice Hall, Englewood Cliffs, NJ, 1986.
11. Pizer, S. M., Amburn, P., Austin, R., Cromartie, R., Geselowitz, A., Geer, T., tar Haar Remeny, J., Zimmerman, J. B., and Zuiderveld, K., Adaptive histogram equalization and its variations. *Comp. Vision Graph. Image Process.* **39**, 355–368 (1987).
12. Restrepo, A., and Bovik, A., An adaptive trimmed mean filter for image restoration. *IEEE Trans. Acoustics, Speech, Signal Process.* **ASSP-36**(8), 8813–8818 (1988).
13. Rosenfeld, A., and Kak, A., *Digital Picture Processing*. Academic Press, New York, 1982.
14. Russ, J. *The Image Processing Handbook*, 2nd Ed. CRC Press, Boca Raton, FL 1994.
15. Sinha, P. K., and Hong, Q. H., An improved median filter. *IEE Trans. Med. Imaging* **MI-9**(3), 345–346 (1990).
16. Wahl, F., *Digital Image Signal Processing*. Artech House, Norwood, MA, 1987.
17. Watkins, C., Sadun, A., and Marenka, A., *Modern Image Processing: Warping, Morphing and Classical Techniques*. Academic Press, London, 1993.